Supporting Information

Ionic Binuclear Ferrocenyl Compounds Containing 1,1,3,3-Tetracyanopropenide Anions. Synthesis, Structural Characterization and Catalytic Effects on Thermal Decomposition of Main Components of Solid Propellants

Dongmei Zhao[a], Jizhen Li[a, b], Fuqiang Bi[b], Yahui Yang[a], Xiaoni Gao[a], Weiqiang Zhang[a], Guofang Zhang[a*] Ziwei Gao[a]

[a] Key Laboratory of Applied Surface and Colloid Chemistry, MOE/School of Chemistry and Chemical Engineering, Shaanxi Normal University, Xi'an 710062, P. R. China

[b] Xi'an Modern Chemistry Research Institute, Xi'an 710065, P. R. China

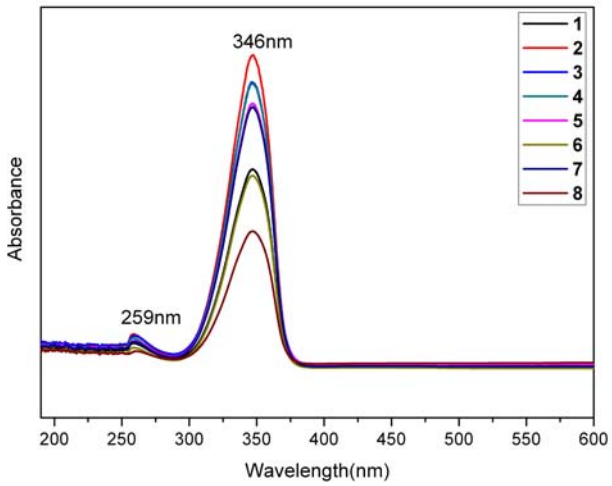

Fig. S1. UV/Vis spectra of compounds **1**−**8** in acetonitrile.

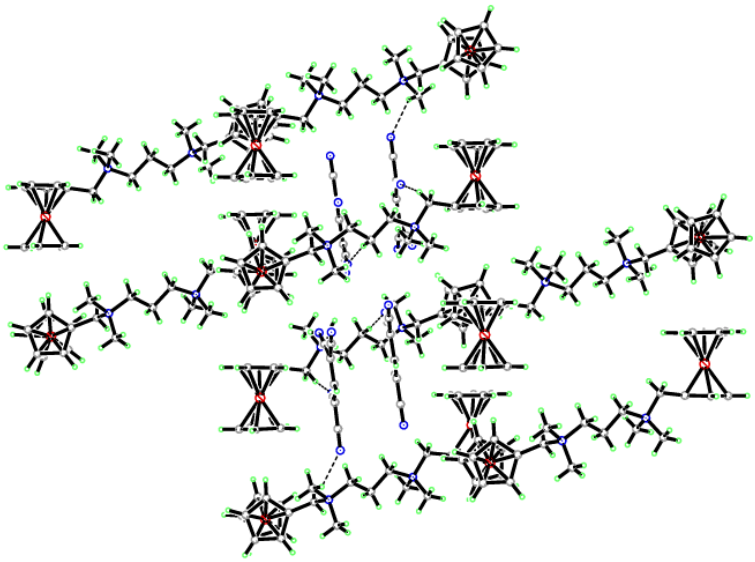

Fig. S2. Crystal structure of **1** as viewed along the *b* axis.

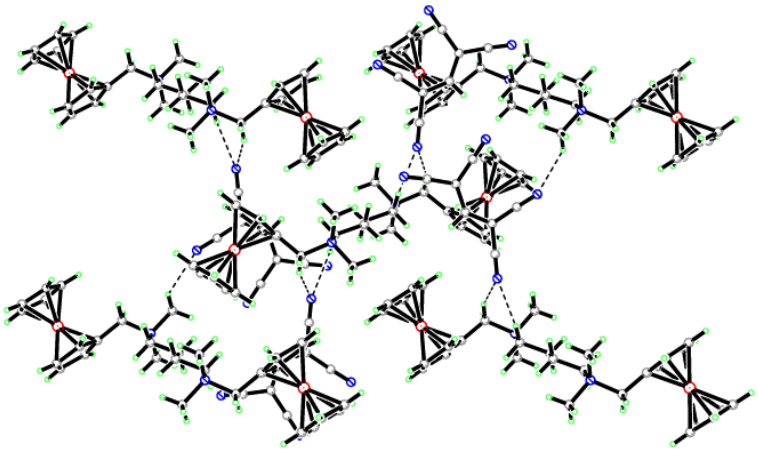

Fig. S3. Crystal structure of **2** as viewed along the *a* axis.

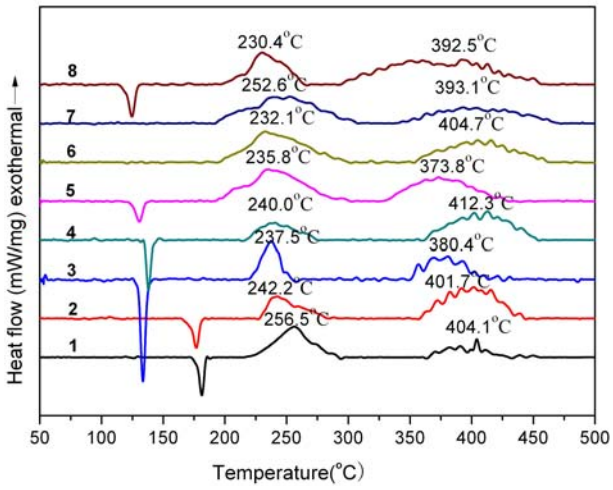

Fig. S4. DSC curves of the new compounds **1**−**8**.

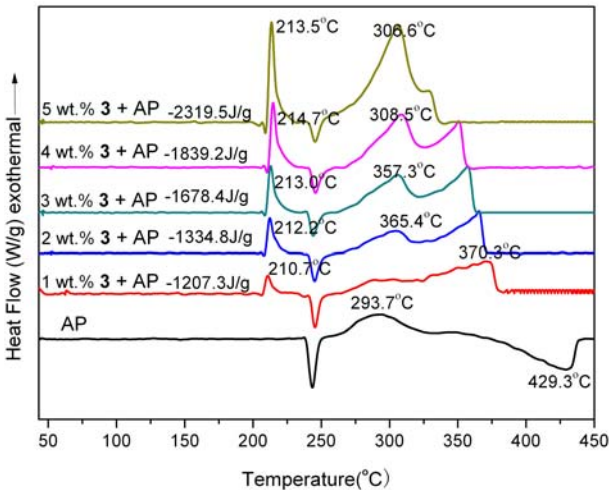

Fig. S5. The DSC curves of pure AP and of the mixtures AP + 1−5 wt.% **1**.

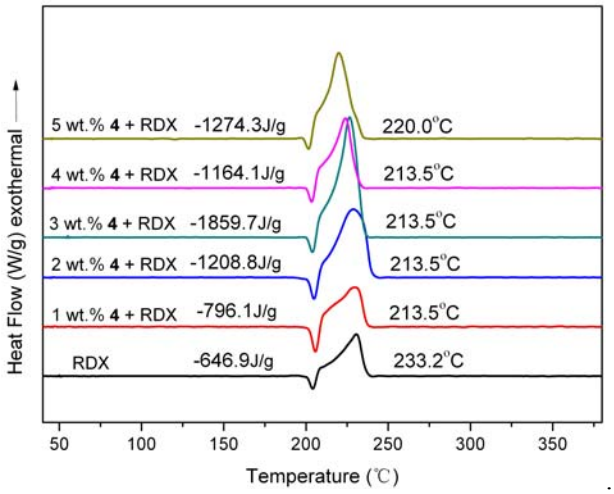

Fig. S6. The DSC curves of pure RDX and of the mixtures RDX + 1−5 wt.% **1**.

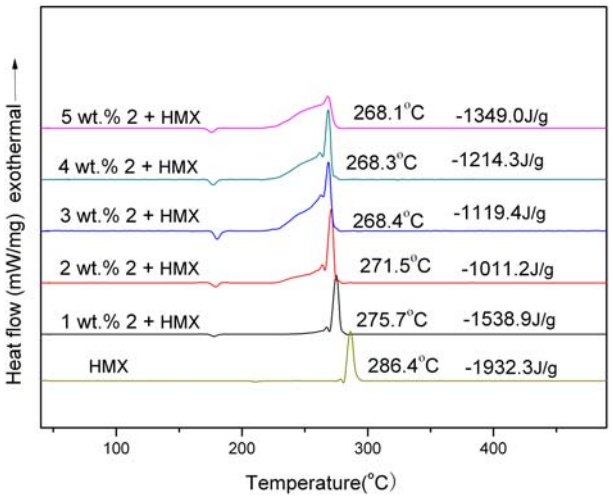

Fig. S7. The DSC curves of pure HMX and of the mixtures HMX + 1−5 wt.% **1**.

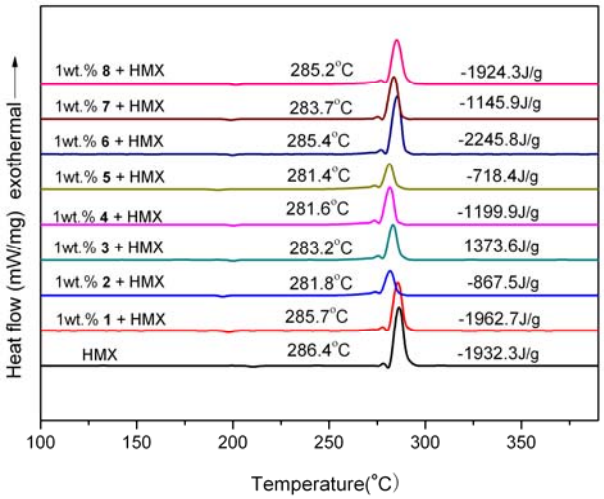

Fig. S8. The DSC curves of pure HMX and of the mixtures HMX + 1 wt.% **1**−**8**.

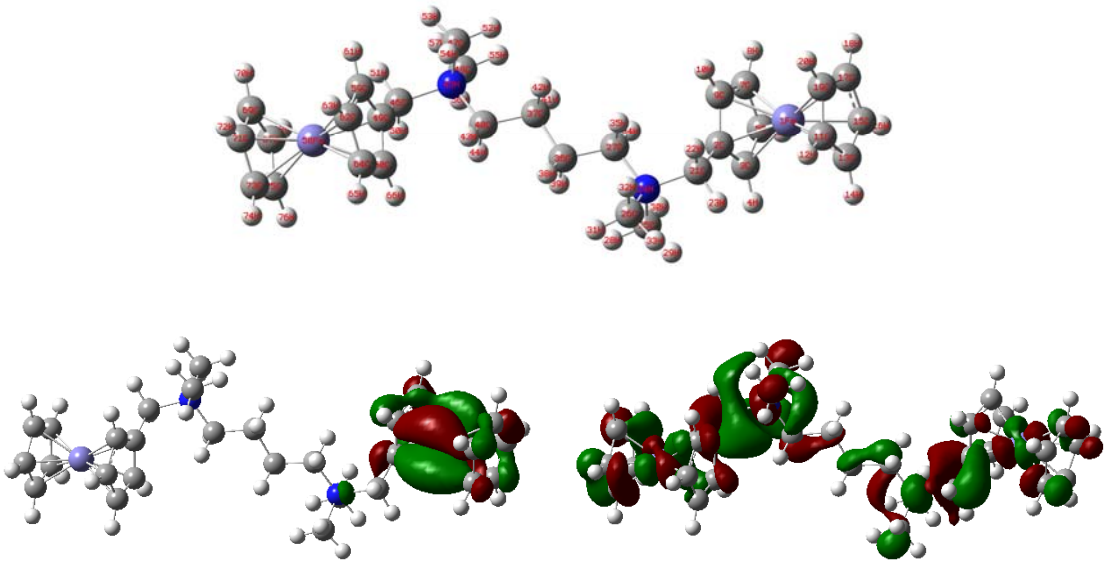

HOMO (133, −10.01 eV) LUMO (134, −5.27 eV)

Fig. S9. The structure of cation of **2** optimized by theoretical calculations (top) and energy diagram of the HOMO (bottom right) and LUMO (bottom left) of the cation of **2**.

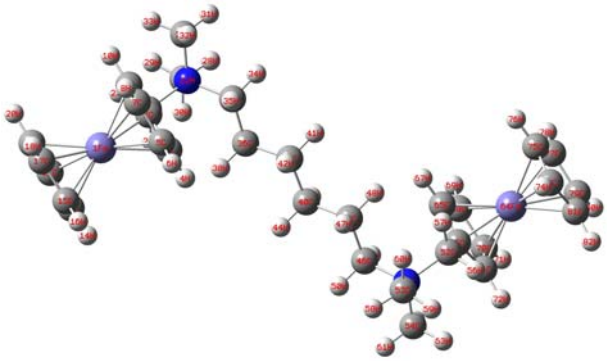

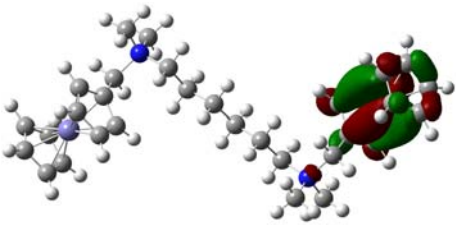

HOMO (87, −9.83 eV)

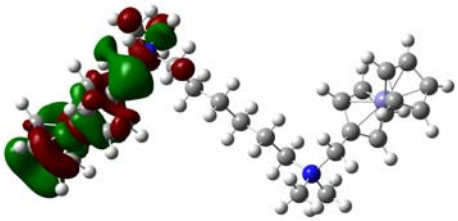

LUMO (88, −4.96 eV)

Fig. S10. The structure of cation of **4** optimized by theoretical calculations (top) and energy diagram of the HOMO (bottom right) and LUMO (bottom left) of the cation of **4**.

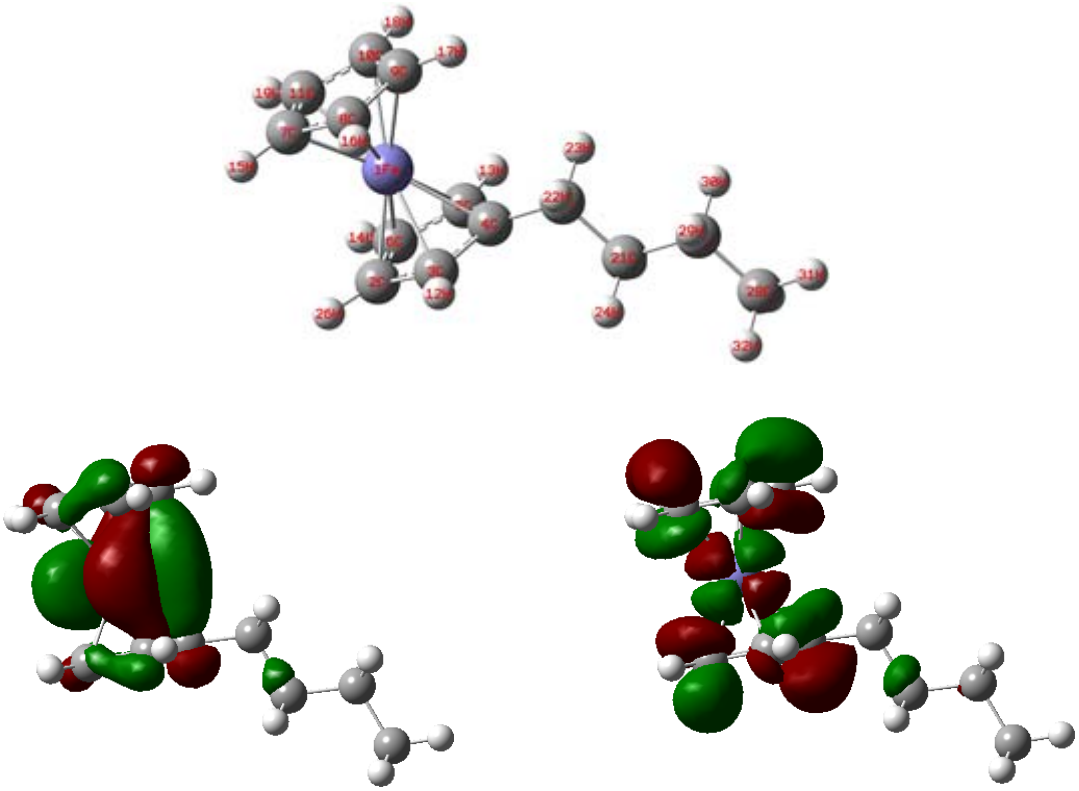

HOMO (59, −5.25 eV)　　LUMO (60, −0.194 eV)

Fig. S11. The structure of **NBF** optimized by theoretical calculations (top) and energy diagram of the HOMO (bottom right) and LUMO (bottom left) of **NBF**.

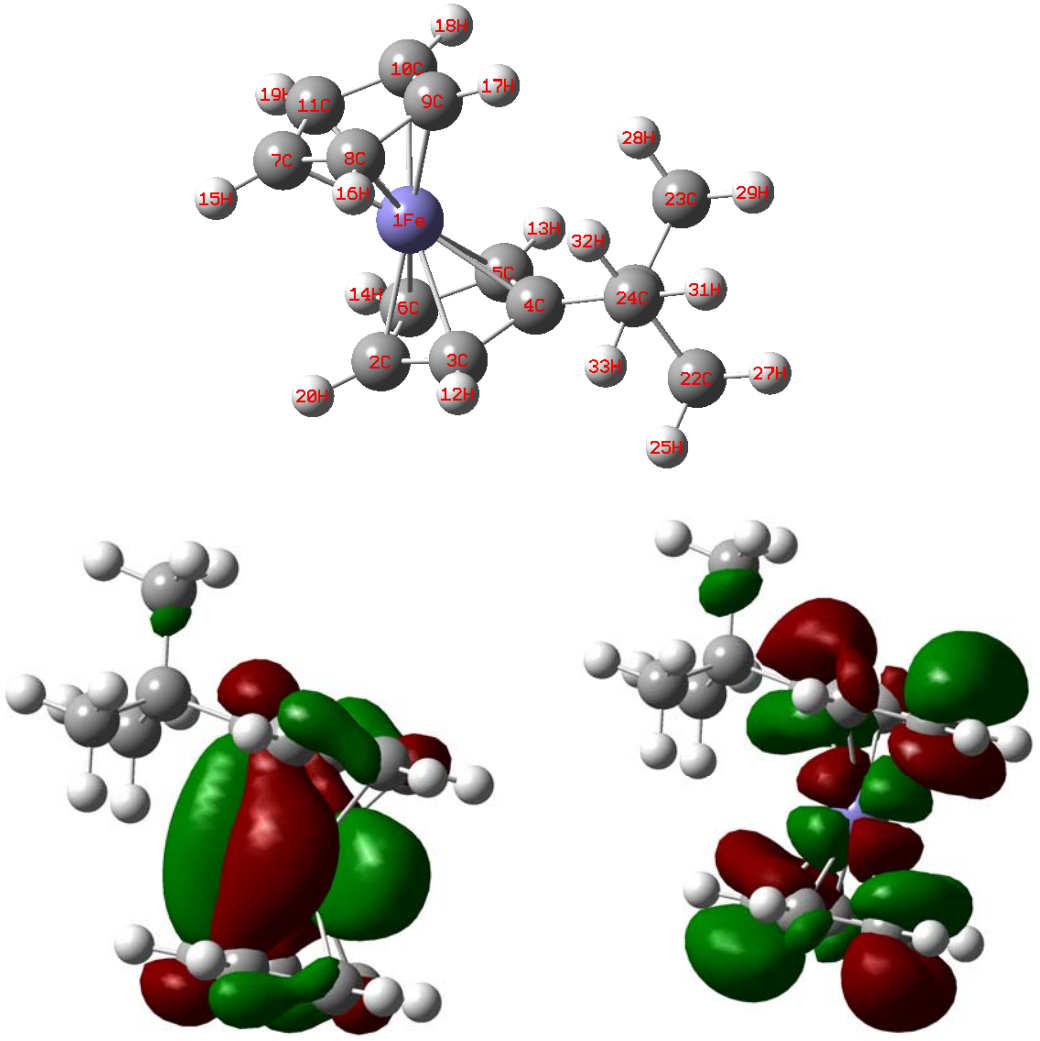

HOMO (59, −5.25 eV) LUMO (60, −0.224 eV)

Fig. S12. The structure of **TBF** optimized by theoretical calculations (top) and energy diagram of the HOMO (bottom right) and LUMO (bottom left) of **TBF**.

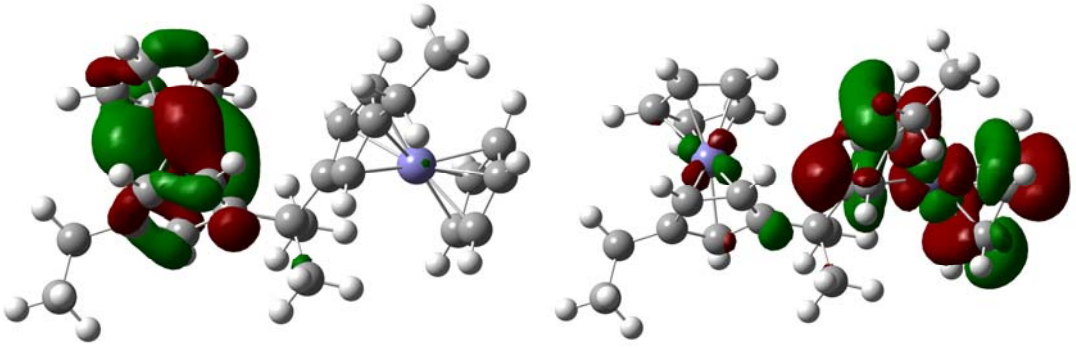

HOMO (113, −5.14 eV)　　LUMO (114, −0.26 eV)

Fig. S13. The structure of **Catocene** optimized by theoretical calculations (top) and energy diagram of the HOMO (bottom right) and LUMO (bottom left) of **Catocene**.

Table S1. Selected bond lengths (Å) and angles (deg) of **1**, **2** and **4**.

		1	
C(30)–C(31)	1.420(4)	C(31)–C(33)	1.379(4)
C(31)–C(32)	1.417(4)	C(33)–C(35)	1.382(3)
C(34)–C(35)	1.422(4)	C(35)–C(36)	1.416(4)
C(30)–N(3)	1.140(3)	C(32)–N(4)	1.141(3)
C(34)–N(5)	1.137(3)	C(36)–N(6)	1.145(4)
C(11)–N(1)	1.526(4)	C(19)–N(2)	1.529(3)
C(33)–C(31)–C(32)	119.1(2)	C(33)–C(31)–C(30)	124.2(2)
C(32)–C(31)–C(30)	116.7(2)	C(31)–C(33)–C(35)	130.2(2)
C(33)–C(35)–C(36)	120.3(2)	C(33)–C(35)–C(34)	124.9(2)
C(36)–C(35)–C(34)	114.7(2)	N(4)–C(32)–C(31)	178.5(3)
N(3)–C(30)–C(31)	179.3(3)	N(6)–C(36)–C(35)	178.5(3)
N(5)–C(34)–C(35)	177.5(3)		
		2	
C(17)–C(19)	1.386(3)	C(19)–C(21)	1.374(3)
C(20)–C(21)	1.415(3)	C(21)–C(22)	1.423(3)
C(16)–C(17)	1.421(3)	C(17)–C(18)	1.427(3)
C(16)–N(2)	1.140(3)	C(18)–N(3)	1.143(3)
C(20)–N(4)	1.143(3)	C(22)–N(5)	1.137(3)
C(11)–N(1)	1.534(3)		
C(19)–C(17)–C(16)	124.7(2)	C(19)–C(17)–C(18)	117.5(2)
C(16)–C(17)–C(18)	117.8(2)	N(3)–C(18)–C(17)	176.3(2)
C(21)–C(19)–C(17)	130.7(2)	N(4)–C(20)–C(21)	177.9(3)
C(19)–C(21)–C(20)	125.4(2)	C(19)–C(21)–C(22)	118.9(2)
C(20)–C(21)–C(22)	115.7(2)	N(5)–C(22)–C(21)	178.9(3)
		4	
N(2)–C(17)	1.136(3)	N(3)–C(19)	1.143(3)
N(4)–C(21)	1.139(3)	N(5)–C(23)	1.147(3)
C(17)–C(18)	1.422(3)	C(18)–C(20)	1.370(3)
C(18)–C(19)	1.423(3)	C(20)–C(22)	1.387(3)
C(21)–C(22)	1.418(3)	C(22)–C(23)	1.419(3)
C(11)–N(1)	1.528(2)		
C(17)–C(18)–C(19)	115.0(2)	C(20)–C(18)–C(19)	119.9(2)
C(20)–C(18)–C(17)	125.1(2)	C(18)–C(20)–C(22)	130.3(2)
C(20)–C(22)–C(21)	124.6(2)	C(20)–C(22)–C(23)	120.5(2)
C(21)–C(22)–C(23)	114.9(2)	N(2)–C(17)–C(18)	177.5(2)
N(3)–C(19)–C(18)	179.4(3)	N(4)–C(21)–C(22)	177.8(2)
N(5)–C(23)–C(22)	179.0(3)		

Note: Symmetry transformations used to generate equivalent atoms. For **2**: #1 1–x, 1–y, 1–z. For **4**: #1 2–x, –y, 1–z.

Table S2. Hydrogen bond parameters for **1**, **2** and **4**.

D–H···A	(D–H) (Å)	(H···A) (Å)	(D···A) (Å)	(D–H···A) (deg)
1				
C(10)–H(10)···N(7)#1	0.98	2.62	3.492(6)	148
C(13)–H(13A)···N(10)#2	0.96	2.44	3.175(4)	133
C(15)–H(15B)···N(3)	0.97	2.56	3.527(4)	175
C(16)–H(16A)···N(6)#2	0.97	2.62	3.474(4)	147
C(19)–H(19B)···N(9)	0.97	2.62	3.489(5)	150
C(33)–H(33)···N(10)#	0.93	2.54	3.456(4)	169
C(40)–H(40)···N(6)#	0.93	2.53	3.418(5)	160
2				
C(11)–H(11A)···N(5)#1	0.98	2.58	3.464(3)	151
C(13)–H(13B)···N(4)#2	0.96	2.59	3.096(3)	113
C(14)–H(14B)···N(5)#1	0.97	2.45	3.376(3)	159
4				
C(7)–H(7)···N(4)#1	0.98	2.60	3.435(4)	143
C(20)–H(20)···N(3)#2	0.93	2.49	3.374(4)	159

Note: Symmetry transformations used to generate equivalent atoms. For **1**: #1 1–x, 1–y, 1–z; #2 1–x ,1–y, –z; #3 2–x, 1–y, –z. For **2**: #1 x, 1/2–y, –1/2+z; #2 1–x, 1/2+y, 1/2–z; #3 1–x ,–1/2+y, 1/2–z. For **4**: #1 x, y, –1+z; #2 2–x, –y, 2–z.

Table S3. Redox potentials from cyclic voltammetry of ferrocenyl groups in **1**–**8**, NBF, TBF and Catocene in 0.1 M *n*-Bu_4PF_6-MeCN

Compd	E_{pa} (mV)	E_{pb} (mV)	$E_p^{1/2}$ (mV)	ΔE_p[a] (mV)
1	681	599	640	82
2	681	590	636	91
3	690	602	646	88
4	680	586	633	94
5	688	599	644	89
6	679	571	625	108
7	681	591	636	90
8	687	596	642	91
NBF	435	353	394	82
TBF	428	327	378	101
Catocene	401, 541	292, 456	347, 499	109, 85

[a] $\Delta E_p = E_{pa} - E_{pb}$